

Analysis of the Absorption Line Profile at 21 cm for the Hydrogen Atom in Interstellar Medium

D. Solovyev

Department of Physics, St. Petersburg State University 198504, St. Petersburg, Russia

E-mail: solovyev.d@gmail.com

Abstract. The paper analyzes the absorption line profile at 21 cm for the hydrogen atom in the interstellar medium. The hydrogen atom is treated as a three-level system illuminated by a powerful light source at neighboring resonances corresponding to the hyperfine splitting of the ground state and Ly_α transition. The field acting upon the resonances gives rise to physical processes, which can be explained as interfering pathways between different transitions. The paper considers particular cases when the 21 cm line profile is substantially modified by the Ly_α transition. A correction to the optical depth is introduced as a result of theory. It is shown that the correction can be considerable and should be taken into account when determining the column density of hydrogen atoms in the interstellar medium. The paper also deals with the effects of none-Doppler broadening and frequency shift.

1. Introduction

Investigation of the interstellar medium (ISM) is of an extreme importance for understanding the factors and mechanisms responsible for the formation of gas clouds and dust complexes and their part in the evolution of stars. Measurements dealing with radio-loud sources can provide information on the structure and physical conditions of galaxies. The observations of hydrogen clouds are the most probable candidate as they cover greater part of the interstellar gas. The 21 cm absorption line in hydrogen atom has a special meaning in investigations of the type, allowing the determination of the distribution and kinematical properties of the neutral hydrogen. Since the direct imaging is restricted by large observing time requirements at all wavebands, the optical imaging studies are complicated [1]. Inasmuch as the interstellar medium is transparent for radio frequencies, this makes the HI 21 cm line the obvious target for the studies.

At the same time, the damped Lyman- α (DLA) systems are of particular interest as the high atomic hydrogen HI column density absorbers. The Lyman α absorption can be used as a very sensitive probe of the HI column in clusters of galaxies [2]. The large cross-section for the Ly α transition makes the technique the most sensitive method for detecting baryons at any redshift [3]. The Lyman- α (whose profile itself is controlled by the kinetic temperature) provides a more effective coupling between the spin temperature and the kinetic temperature for the high density cloud illuminated by a powerful source of light [4]. The damping wings of the Lorentzian component of the absorption profile become possible to be detected from about the $\sim 10^{19} \text{ cm}^{-2}$ column density, attaining their maximum in the "damped Ly α systems" [3]. At low densities of the ISM, collisions are inefficient for lowering the spin temperature. If Lyman alpha radiation penetrates the HI without heating it, it can actually lower the spin temperature so that the 21 cm line becomes a stronger absorption feature. Thus, the 21 cm absorption and Ly α absorption line profiles provide two independent tools for the investigation of ISM. Yet, investigation in the absorption 21 cm and Ly α lines cannot be considered separately. For example, author of [5] has considered the populations of the magnetic sublevels for the hyperfine splitting of the ground state $2s_{1/2}$ in hydrogen atom, whereas [5] investigated the atomic orientation depending on the intensity, spectrum, angular distribution, and polarization of the incident optical and radio emission.

In view of the above, the paper focuses on the interstellar neutral hydrogen atom subjected to an external field at frequencies of hyperfine energy splitting of the ground state, 21 cm, and the Ly α transition. Description of such atom-field system can be reduced to the examination of the three-level atom. The main constraints in our analysis arise due to describing the hyperfine structure of the ground state without the account for the fine and hyperfine structure of the excited $2p$ state. However, the approximation can be justified by a large value of the Ly α transition rate and approximate equivalence of the one-photon $1s \leftrightarrow 2p$ transition probabilities between the fine and hyperfine sublevels in the hydrogen atom.

The paper provides a detailed analysis of the absorption profile at 21 cm line for

the hydrogen atom in the interstellar medium. To this end, the atom-field system is described within the framework of density matrix formalism [6]. The hydrogen atom is treated as a three-level ladder (cascade) system: two hyperfine sublevels of the ground atomic state and excited $2p$ state, see Fig. 1. The unperturbed 21 cm line profile is

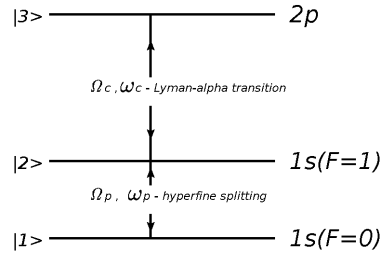


Figure 1. Schematic representation of energy levels in a hydrogen atom. The lower states correspond to the ground state with the hyperfine sublevels for the total angular momenta $F = 1$ and $F = 0$. The frequency of the transition between the hyperfine sublevels is 21 cm. The upper state is the $2p$ excited state corresponding to the Lyman- α transition. Ω_p and Ω_c denote the corresponding Rabi frequencies for the probe and controlled fields of the external source.

shown to arise at a negligible field strength of the neighboring transition ($\Omega_c \rightarrow 0$). However, the profile can be modified significantly by the Ly_α transition induced in the field of a powerful light source. In this case, the absorption process cannot be thought of as a one-photon transition between the hyperfine sublevels of the ground state in the hydrogen atom. The developed theory allows finding a correction to the optical depth. The correction correlates directly with the determination of the column density of hydrogen atom in the interstellar medium. The paper presents certain events where the correction is of significance, some of them just illustrating the importance of the analysis.

2. Correction to the optical depth via the evaluation of three-level Ξ scheme

Recently, the density matrix formalism was applied to study the effect of Electromagnetically-Induced Transparency (EIT) in hydrogen atom under the conditions corresponding to the recombination era of the universe [7, 8]. It was shown that the EIT phenomenon could lead to corrections on the order of 1% in the observed cosmic microwave background (CMB). To study the absorption line profile corresponding to the 21 cm transition in hydrogen atom, the present work draws on the same formalism.

Theoretical description of an atom within the three-level cascade Ξ -scheme approximation can be found in [9, 10], which employed the density matrix formalism. The example of the rubidium atom was used to investigate the EIT phenomenon in [11], where the physical picture of the effect was rendered in terms of interfering multiphoton transition pathways. Basing on the formalism given in [9]-[11], the influence of EIT phenomenon on the optical depth determination for the interstellar hydrogen atom is

investigated. The three-level Ξ scheme in hydrogen atom with the energy levels: state $|1\rangle$ is the lower and state $|2\rangle$ is the upper hyperfine sublevels of the ground $1s$ state, with state $|3\rangle$ representing the excited $2p$ level in the hydrogen atom. The absorber is assumed to be subjected to the "probe" and "controlled" fields with the corresponding frequencies $\omega_p \rightarrow \omega_{21} = |1\rangle \leftrightarrow |2\rangle$ and the Ly_α transition $\omega_c \rightarrow \omega_{32} = |2\rangle \leftrightarrow |3\rangle$.

The set of equations for the ladder scheme is

$$\begin{aligned}\rho_{21} &= \frac{i/2 (\Omega_p(\rho_{22} - \rho_{11}) - \Omega_c^* \rho_{31})}{\gamma_{21} - i\delta_p}, \\ \rho_{32} &= \frac{i/2 (\Omega_c(\rho_{33} - \rho_{22}) + \Omega_p^* \rho_{31})}{\gamma_{32} - i\delta_c}, \\ \rho_{31} &= \frac{i/2 (\Omega_p \rho_{32} - \Omega_c \rho_{21})}{\gamma_{31} - i(\delta_p + \delta_c)}, \\ \rho_{22} &= \frac{i}{2\Gamma_2} (\Omega_p^* \rho_{21} - \Omega_p \rho_{12}), \\ \rho_{33} &= \frac{i}{2\Gamma_3} (\Omega_c^* \rho_{32} - \Omega_c \rho_{23}),\end{aligned}\tag{1}$$

where detunings for the probe and controlled fields are $\delta_p = \omega_p - \omega_{21}$, $\delta_c = \omega_c - \omega_{32}$, respectively, and ω_{21} , ω_{32} represent the exact values of corresponding transitions. The Rabi frequencies are denoted with $\Omega_c = 2d_{32}E_c/\hbar$ and $\Omega_p = 2\mu_{21}B_p/\hbar$. Since the transition between the hyperfine sublevels corresponds to the magnetic dipole M1 emission/absorption, Rabi frequency Ω_p is written in terms of magnetic field strength B_p and magnetic moment μ_{ij} . E_c represents the electric field strength for Ly_α transition and d_{ij} is the dipole matrix element. The wave functions for $|3\rangle$, $|2\rangle$, and $|1\rangle$ states can be taken as the solution of Schrödinger equation. In the absence of collisions, $\gamma_{ij} = (\Gamma_i + \Gamma_j)/2$, where Γ_i is the natural width of the i th level. The set of equations (1) is written in the steady-state and rotating wave approximations, see [9]-[11].

With the use of Eqs. (1), the monochromatic absorption coefficient at frequency ω_{ij} can be defined as

$$k = \frac{N d_{ij}^2 \omega_{ij}}{2\varepsilon_0 \Omega_{ij}} \text{Im}\{\rho_{ij}\},\tag{2}$$

where ε_0 is the vacuum permittivity, N is the number of atoms and Ω_{ij} is the corresponding Rabi frequency. Taking into account the relation $k = \tilde{k}\phi(\omega)$, where \tilde{k} is the integrated line absorption coefficient and $\phi(\omega)$ is the normalized line profile, the monochromatic optical depth is

$$d\tau(\omega_{ij}) = -\tilde{k}\phi(\omega_{ij})dl = -\tau\phi(\omega_{ij})\frac{dl}{L},\tag{3}$$

where l is the distance along the ray [12].

In ordinary case the monochromatic optical depth corresponds to the one-photon resonant process that reduces to the evaluation of the two-level atomic system. Then the one-photon absorption process is described by the Lorentz line profile:

$$\text{Im}\{\rho_{21}^{(0)}\} = -\frac{\gamma_{21}\Omega_p/2}{\delta_p^2 + \gamma_{21}^2},\tag{4}$$

where δ_p can be considered as a variable. A more accurate solution of Eqs. (1) corresponds to accounting of the second field acting upon the adjacent resonance. Then, in the limit of the weak "probe" field [10], matrix element ρ_{21} in the first order of the "probe" field and in all orders of the "control" field is

$$\rho_{21} = \frac{i\Omega_p/2}{i\delta_p - \gamma_{21} + \frac{\Omega_c^2/4}{i(\delta_p + \delta_c) - \gamma_{31}}}. \quad (5)$$

Expression (5) depends on field parameters Ω_c and δ_c and reduces to Eq. (4) in the limit $\Omega_c \rightarrow 0$, i.e. when the influence of the field on adjacent resonance is negligible. In this case, the corrections to 'ordinary' determination (4) can be found via the series expansion in $\Omega_{p(c)}$ at zero detunings $\delta_{p(c)}$. Then the transition amplitudes associated with $|1\rangle \rightarrow |2\rangle$ and $|2\rangle \rightarrow |3\rangle$ pathways result in the destructive interference and the reduction of the total probability that a probe photon will be absorbed [11].

However, the series expansion in Rabi frequencies cannot be employed in our case due to the smallness of level width $\Gamma_2 \approx 2.85 \cdot 10^{-15} \text{ s}^{-1}$. Nonetheless, the imaginary part of ρ_{21} can be separated out

$$\begin{aligned} -Im\{\rho_{21}\} &\equiv -Im\{\rho_{21}^{(1)}\} - Im\{\rho_{21}^{(2)}\} = \\ &\frac{\gamma_{21}\Omega_p/2}{\left(\delta_p - \frac{(\delta_p + \delta_c)\Omega_c^2/4}{(\delta_p + \delta_c)^2 + \gamma_{31}^2}\right)^2 + \left(\gamma_{21} + \frac{\gamma_{31}\Omega_c^2/4}{(\delta_p + \delta_c)^2 + \gamma_{31}^2}\right)^2} + \\ &\frac{\gamma_{31}\Omega_p\Omega_c^2/8}{\left[\left(\delta_p - \frac{(\delta_p + \delta_c)\Omega_c^2/4}{(\delta_p + \delta_c)^2 + \gamma_{31}^2}\right)^2 + \left(\gamma_{21} + \frac{\gamma_{31}\Omega_c^2/4}{(\delta_p + \delta_c)^2 + \gamma_{31}^2}\right)^2\right] ((\delta_p + \delta_c)^2 + \gamma_{31}^2)}. \end{aligned} \quad (6)$$

The first term here represents the one-photon $|1\rangle \rightarrow |2\rangle$ (21 cm) absorption process, the second term can be associated with the additional process $|1\rangle \rightarrow |2\rangle \rightarrow |3\rangle \rightarrow |2\rangle$ [11]. In absence of the second field $\Omega_c = 0$, the second term in Eq. (6) vanishes, and the ordinary definition (4) can be found. The line profiles corresponding to Eqs. (4) and (6) are given schematically in Figs. 2 and 3, respectively. In particular, Figs. 2 and 3 show that the contribution arising via the additional pathways leads to the distortion the line profile in the vicinity of zero detuning δ_c .

Thus, the absorption coefficient and the optical depth, respectively, cannot be described by the single Lorentz contour Eq. (4) with the subsequent transformation to the Voigt profile. The Voigt fitting, in this case, is the overabundant and covers the physical processes occurring in the medium illuminated with the radiation from a powerful light source at the adjacent resonances. It can be noted also that the first term corresponding to the absorption at 21 cm line ($|1\rangle \rightarrow |2\rangle$ transition) shows the line profile to be broadened and shifted *a priori*.

The dimensionless correction to the optical depth Eq. (3) arising in context of Eq. (6) can be defined as follows

$$\tau = \tau_0(1 + \delta\tau), \quad (7)$$

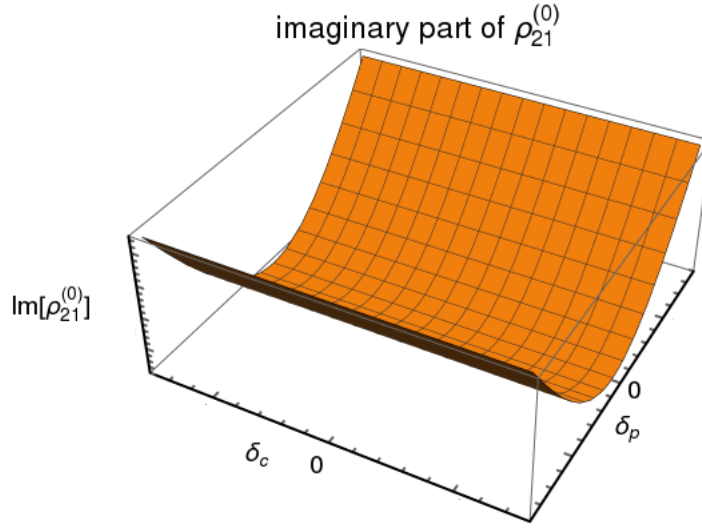


Figure 2. Schematic image of the line profile corresponding to $Im\{\rho_{21}^{(0)}\}$, Eq. (4), for different values of detunings δ_p and δ_c .

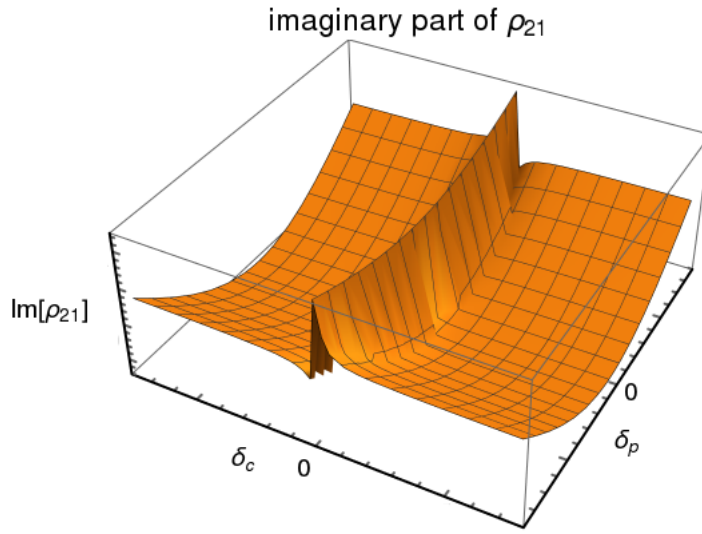


Figure 3. Schematic image of the line profile corresponding to $Im\{\rho_{21}\}$, Eq. (6), for different values of detunings δ_p and δ_c .

where τ_0 corresponds to single profile $Im\{\rho_{21}^{(1)}\}$ and correction $\delta\tau$ is

$$\delta\tau = \frac{Im\{\rho_{21}\} - Im\{\rho_{21}^{(1)}\}}{Im\{\rho_{21}^{(1)}\}} \equiv \frac{Im\{\rho_{21}^{(2)}\}}{Im\{\rho_{21}^{(1)}\}}. \quad (8)$$

Expression (8) simplifies to

$$\delta\tau = \frac{\gamma_{31}}{\gamma_{21}} \frac{\Omega_c^2}{4((\delta_p + \delta_c)^2 + \gamma_{31}^2)}. \quad (9)$$

Note that the expression (9) is of a resonant nature but independent of probe field Ω_p acting on the 21 cm line.

3. None-Doppler broadening and frequency shift

The section deals with the effects of absorption line broadening and frequency shift for an atom at rest and assumption of Ω_c smallness.

3.1. None-Doppler broadening

The non-Doppler line broadening for the $|1\rangle \rightarrow |2\rangle$ transition follows from the denominator in the first term and is proportional to Ω_c . This broadening can be expressed as an additional term to natural width γ_{21} :

$$\gamma = \gamma_{21} + \frac{\gamma_{31}\Omega_c^2/4}{(\delta_p + \delta_c)^2 + \gamma_{31}^2} = \gamma_{21} + \gamma_{\text{broad}}. \quad (10)$$

The maximum value of γ_{broad} is attained for the exact two-photon resonance $\delta_p + \delta_c = 0$:

$$\gamma_{\text{broad}} = \frac{\Omega_c^2}{4\gamma_{31}}. \quad (11)$$

For very powerful light source and small distances between the absorber and the source, it can be expected that the value of γ_{broad} is possibly larger than natural level width γ_{21} .

Taking into account the motion of interstellar gas cloud, we can find that the resonant frequency should be shifted. This Doppler shift leads to $\delta_c \rightarrow \delta_c + \frac{v}{c}\omega_c$ [11], where c is the speed of light. The speed of hydrogen clouds can be on the order of few hundreds $km \cdot s^{-1}$ [13], [14] and, in some cases, as high as thousand kilometers per second [15]. Then the sum of detunings $\delta_p + \delta_c$ can be estimated as $(10^{-3} - 10^{-2})\omega_c \sim (10^4 - 10^5)\gamma_{31}$, where $\gamma_{31} = \frac{1}{2}\Gamma_{2p} = \frac{1}{2}6.265 \cdot 10^8 s^{-1}$ and Ly_α frequency is $\omega_c = 2.466 \cdot 10^{15} s^{-1}$. Thus, the Doppler shift leads to the suppression of γ_{broad} . Nonetheless, since the emission spectrum of the source is of a continuum nature, the case of the exact two-photon resonance can always be singled out. It should be underscored that this discussion corresponds to γ_{broad} and does not cancel the Doppler broadening leading to the Voigt profile.

3.2. Frequency shift

Equation (6) allows also finding the frequency shift for the transition $|1\rangle \rightarrow |2\rangle$. To this end, detuning δ_p can be considered as the 'scanning' parameter (variable). Then the resonance condition reads

$$\delta_p - \frac{(\delta_p + \delta_c)\Omega_c^2/4}{(\delta_p + \delta_c)^2 + \gamma_{31}^2} = 0. \quad (12)$$

Now, the frequency shift is zero for the exact two-photon resonance, $\delta_p + \delta_c = 0$. In case, when the detuning of the two-photon resonance $\delta_p + \delta_c = \gamma_{31}/2$, the frequency shift can be found as

$$\delta_{\text{shift}} = \frac{\Omega_c^2}{4\gamma_{31}}. \quad (13)$$

Here, level width γ_{31} acts as a natural parameter for the atomic resonant excitation.

Another result arises in the assumption that $\delta_p \sim \gamma_{21} \ll \delta_c \sim \gamma_{31}$ (one-photon resonances). Then, neglecting δ_p in the second term of Eq. (12), the frequency shift is

$$\delta_{\text{shift}} = \frac{\delta_c \Omega_c^2}{4\delta_c^2 + 4\gamma_{31}^2}. \quad (14)$$

Here, we can take into account the motion of hydrogen cloud by using parameter β : $\delta_c = v/c \cdot \omega_c \equiv \beta\gamma_{31}$. Therefore,

$$\delta_{\text{shift}}^\beta = \frac{\Omega_c^2}{4\gamma_{31}} \frac{\beta}{1 + \beta^2} \approx \frac{\Omega_c^2}{4\gamma_{31}} \frac{1}{\beta}. \quad (15)$$

The shift is negligibly small, and the maximum shift can be attained for the two-photon resonance with the detuning being $\delta_p + \delta_c = \gamma_{31}/2$, see Eq. (13).

4. Numerical results

To evaluate the contribution of non-Doppler broadening, frequency shift and correction to the optical depth, see Eqs. (11), (14) and (9), respectively, one is to find Rabi frequency Ω_c . It can be done via the flux density or luminosity of the light sources and the distance between the source and the absorber. To this end, the observation data of Damped Lyman- α systems at 1216 Å line in hydrogen [15], [16]-[31] were used. Finding the distance employed the following expression:

$$r = \frac{c}{H_0}(z_{\text{em}} - z_{\text{abs}}), \quad (16)$$

where $H_0 = 2.3 \cdot 10^{-18} s^{-1}$ is the Hubble constant, z_{em} , z_{abs} are the redshifts of the source and the absorber, respectively. The radiation intensity at the absorber can be defined as

$$I_{\text{abs}} = \frac{L_*}{4\pi(1 + z_{\text{em}} - z_{\text{abs}})^4 r^2}, \quad (17)$$

where L_* is the star luminosity (measured in units of W/Hz), which is independent of the distance. For observed flux density S at frequency ν , the intensity at the absorber is

$$S_{\text{abs}} = S_0 \nu_0 \frac{z_{\text{em}}^2 (1 + z_{\text{em}})^4}{(z_{\text{em}} - z_{\text{abs}})^2 (1 + z_{\text{em}} - z_{\text{abs}})^4}, \quad (18)$$

where S_0 is the measured flux density and ν_0 is the frequency of the corresponding transition.

The flux density for the Ly α line can be expressed via electric field strength E_α as

$$S_\alpha = \frac{1}{2} \sqrt{\frac{\epsilon_0}{\mu_0}} c E_c^2, \quad (19)$$

where ϵ_0 is the vacuum permittivity and μ_0 is the vacuum permeability. In principle, the Rabi frequency for the 21 cm transition can be defined in the same way, i.e. as $S_{21} = \frac{1}{2} \sqrt{\frac{\epsilon_0}{\mu_0}} c B_p^2$. The data used in our calculations are collected in Table 1.

Table 1. The first column contains the names of sources. The second and third columns represent the redshift of the star and the absorber, respectively, where the 21 cm absorption in conjunction with Ly $_{\alpha}$ absorption were observed. The next column shows the density flux at 1.4 GHz frequency (hyperfine splitting of the ground state in hydrogen atom, $|1\rangle \leftrightarrow |2\rangle$ transition in the present calculations). The fifth column lists the values of density flux and luminosity at Ly $_{\alpha}$ frequency. The values of the hydrogen velocity at 21 cm line are given in the sixth column. Finally, the optical depth values are given in the last column of the table. References with the data used are given in square brackets.

^a The component with the poorest accuracy is taken from [21].

^b Just one of components from [29] is considered.

^c Cloud 3 is treated in accordance to data [31].

^d optical depth at the Lyman-limit [39].

Name	z_{em}	z_{abs}	$S_{1.4GHz}, Jy$	$\log L_{\alpha}, (W \cdot Hz^{-1})$	$v, (km \cdot s^{-1})$	τ_0
0235+164	0.94	0.523869	1.7[16]	$\log[\nu f] \approx -12.5[17]$	125[18]	$(\frac{1}{T}) \int \tau dv = 13 \pm 0.6[18]$
3C 190	1.1946	1.19565	2.47[19]	0.17 Jy[19]	-37.1[21]	$0.0027 \pm 0.0002[21]^a$
3C 216	0.668	0.63	3.4[19]	22.699[20]	102[22, 15]	0.38[23]
J0414+0534	2.6365	0.9586	1.82[24]	22.188[20]	205[25]	0.0212(16)[25]
J0414+0534	2.6365	2.63534	3.31[26]	22.188[26]	-94[26]	$(0.015 \pm 0.002)[26]$
0902+343	3.398	3.3968	1.2[27]	22.422[20]	120[27, 28]	-
3C 49	0.621	0.6207	7.28[29]	20.777[20]	-138[29]	$0.036 \pm 0.003[29]^b$
3C 286	0.849	0.692153	14.7[19]	2.7 Jy [19]	4.2[31]	$0.280 \pm 0.004[31]^c$
0118-272	0.559	0.558	0.93[19]	0.95 Jy [19]	-	$\log[N_{HI}] = 20.3[19]$
0405-331	2.570	2.562	0.63[32]	0.56 Jy [32]	-	$\log[N_{HI}] = 20.6[32]$
0537-286	3.104	2.976	0.862[19]	0.90 Jy [19]	-	$(0.41 \pm 0.22) \cdot 10^{22}$
0957+561A	1.413	1.391	0.59[19]	0.15 Jy [19]	25 [33]	$N_{HI} = 7 \cdot 10^{19} \pm 30\% [34]$
0248+430	1.31	0.3939	1.4[19]	1.5 Jy [19]	40 [35]	$N_{HI} = (3.6 \pm 0.4) \cdot 10^{19}$
0336-017	3.197	3.0619	0.60[19]	0.15 Jy [19]	13	$\log[N_{HI}] = 21.25, \tau_0 < 0.2 [36]$
0528-250	2.813	2.8110	1.16[19]	0.59 Jy [19]	5 [37]	$\log[N_{HI}] = 21.3 \pm 0.1 [38]$
2128-123	0.501	0.430	1.8[19]	0.7 Jy [19]	75 [39]	$\log[N_{HI}] = 19.37 \pm 0.08, \tau_{LL} \simeq 150[39]^d$

Employing equations (17)-(19) and data from Table 1, the line broadening and the frequency shift were evaluated with Eq. (11) and Eq. (15), respectively. The correction to optical depth $\delta\tau$ for the zero and non-zero detunings are calculated with Eq. (9). The Doppler effect can be taken into account with the use of data in Table 1 (sixth column). It should be pointed out that in view of smallness of frequency ω_{21} in respect to Ly $_{\alpha}$, detuning δ_p can be set equal to zero, since $\delta_p = \beta\omega_p \ll \delta_c = \beta\omega_c$. The results of the numerical calculations are given in Table 2, notations $\delta\tau_0$ and $\delta\tau$ corresponding to the zero and non-zero detunings, respectively.

5. Analysis of results

Typically, astrophysical investigations of absorption lines employ the one-photon profile. Within the framework of density matrix formalism, the one-photon absorption line profile can be derived in the two-level approximation, see Eq. (4), for the atom in an external field. According to the approximation, the monochromatic absorption coefficient and, hence, the optical depth can be defined via the imaginary part of the density matrix element, Eqs. (2), (3). In this case, the definition of the optical depth and all the ensuing physical quantities leads to the results of the 'ordinary' theory. However, section 2 demonstrated that this was the case of the zeroth approximation, when the

Table 2. The first column contains the name of sources in correspondence to the Table 1. The second column gives the values evaluated with Eq. (11) for the non-Doppler broadening. Frequency shift $\delta_{\text{shift}}^{\beta}$ Eq. (15) for the $|1\rangle \leftrightarrow |2\rangle$ transition is represented in the third column. The fourth column lists the relative contributions of $\delta\tau$ at detunings $\delta_p \ll \delta_c = \frac{v}{c}\omega_{32}$. Values of $\delta\tau_0$ are given in the last column, in which the second subrow contains the values of correction to the optical depth listed in Table 1.

Name	γ_{broad} in s^{-1} Eq. (11) $v s \Gamma_2 = 2.85 \cdot 10^{-15} s^{-1}$	$\delta_{\text{shift}}^{\beta}$ in s^{-1} Eq. (15)	$\delta\tau$ at $\delta_c = \frac{v}{c}\omega_{32}$	$\delta\tau_0$ $\delta\tau_0 \cdot \tau_0$
0235+164	$9.28 \cdot 10^{-20}$	$3.87 \cdot 10^{-23}$	$1.53 \cdot 10^{-13}$	$6.51 \cdot 10^{-5}$ $8.46 \cdot 10^{-4}$
3C 216	$2.34 \cdot 10^{-17}$	$7.97 \cdot 10^{-21}$	$5.805 \cdot 10^{-11}$	0.0164 $6.23 \cdot 10^{-3}$
J0414+0534 $z_{\text{abs}} = 0.9586$	$4.93 \cdot 10^{-24}$	$3.37 \cdot 10^{-27}$	$3.02 \cdot 10^{-18}$	$3.46 \cdot 10^{-9}$ $7.33 \cdot 10^{-11}$
J0414+0534 $z_{\text{abs}} = 2.63534$	$5.59 \cdot 10^{-16}$	$1.75 \cdot 10^{-19}$	$1.63 \cdot 10^{-9}$	0.392 $5.88 \cdot 10^{-3}$
0902+343	$8.502 \cdot 10^{-16}$	$3.403 \cdot 10^{-19}$	$1.52 \cdot 10^{-9}$	0.597
3C 49	$3.07 \cdot 10^{-16}$	$1.41 \cdot 10^{-19}$	$4.15 \cdot 10^{-10}$	0.215 $7.74 \cdot 10^{-3}$
0248+430	$6.38 \cdot 10^{-16}$	$8.51 \cdot 10^{-20}$	$1.03 \cdot 10^{-8}$	0.448 –
2128-123	$1.32 \cdot 10^{-14}$	$3.31 \cdot 10^{-18}$	$6.07 \cdot 10^{-8}$	0.108 16.1
3C 190	$3.08 \cdot 10^{-11}$	$3.798 \cdot 10^{-15}$	$5.79 \cdot 10^{-4}$	$4.63 \cdot 10^{-5}$ $1.25 \cdot 10^{-7}$
3C 286	$8.398 \cdot 10^{-14}$	$1.18 \cdot 10^{-18}$	$1.23 \cdot 10^{-4}$	0.0169 0.00475
0118-272	$1.72 \cdot 10^{-10}$	–	–	$8.29 \cdot 10^{-6}$ –
0405-331	$8.95 \cdot 10^{-10}$	–	–	$1.59 \cdot 10^{-6}$ –
0537-286	$2.07 \cdot 10^{-11}$	–	–	$6.88 \cdot 10^{-5}$ –
0957+561A	$1.89 \cdot 10^{-12}$	$1.58 \cdot 10^{-16}$	$7.81 \cdot 10^{-5}$	$7.53 \cdot 10^{-4}$ 0.0753
0336-017	$3.69 \cdot 10^{-12}$	$1.60 \cdot 10^{-16}$	$5.63 \cdot 10^{-4}$	$3.86 \cdot 10^{-4}$ $7.72 \cdot 10^{-5}$
0528-250	$2.41 \cdot 10^{-8}$	$4.02 \cdot 10^{-13}$	0.0402	$5.91 \cdot 10^{-8}$ –

one-photon absorption process is considered for an isolated transition in the atom. Accounting for the absorption/emission processes that occur at adjacent transitions leads to a substantial modification of the line profile. The paper employs the three-level approximation for the atom. Within the theory [7]-[11], the imaginary part of a density matrix element fails to correspond to the isolated transition and strongly depends on field parameters defined for the adjacent resonance, Eq. (5).

5.1. Correction to the optical depth

The absorption line profile of the $|1\rangle \leftrightarrow |2\rangle$ transition is shown in the paper to be formed by two contributions: $Im\{\rho_{21}^{(1)}\}$ and $Im\{\rho_{21}^{(2)}\}$, see Eq. (6). The additional term in the line profile is proportional to Ω_p and Ω_c , Rabi frequencies of the $|1\rangle \leftrightarrow |2\rangle$ and $|2\rangle \leftrightarrow |3\rangle$ transitions, respectively. Its physical interpretation was given in [11] as the interfering emission/absorption pathways in an atom. Using such modification, the correction to the optical depth can be found as Eq. (9). The correction should be small for $\Omega_c \ll \gamma_{21}$. However, in view of smallness of level width γ_{21} , the condition is met for very distant source and absorber, while the opposite situation can be found for $z_{em} \approx z_{abs}$ and a very powerful source of light. In this case, the main contribution to the line profile comes from the second term $Im\{\rho_{21}^{(2)}\}$, and the correction to the optical depth should be taken as the reciprocal value of the former one. Numerical results for the correction to the optical depth at zero detunings in case of $\Omega_c \ll \gamma_{21}$ and $\gamma_{21} \ll \Omega_c$ are collected in the first and second parts of Table 2 as $\delta\tau_0$, respectively.

Although the case of zero detuning can be always singled out, since the light source emission is of the continuum nature, the velocity of clouds can be taken into account for the detailed description of the 21 cm absorption line profile ($|1\rangle \leftrightarrow |2\rangle$ transition) in the interstellar medium. This can be rendered by the approximate equality $\delta_p + \delta_c \approx \frac{v}{c}\omega_{32}$, where values of v are listed in Table 1. Numerical results for $\delta\tau$ are also given in Table 2.

In particular, it follows from Table 2 that the contribution of $\delta\tau_0$ can be significant and exceed the accuracy of the experimental determination of τ_0 . Although our analysis is rather rough and does not include the Voigt profile fitting, the main conclusion is that the two-level approximation of atom is insufficient. Already in the three-level approximation, the additional processes occurring in the atom should be taken into consideration in the appropriate fitting of the absorption profile. The parameters of medium extracted from such fitting can be corrected with use of Eqs. (6), (9).

5.2. None-Doppler broadening and frequency shift

In keeping with Eq. (6), the absorption line profile can be analyzed in terms of line broadening. Without regard to which contribution is dominant, $Im\{\rho_{21}^{(1)}\}$ or $Im\{\rho_{21}^{(2)}\}$, the absorption line derived via the density matrix element is modified by width γ_{broad} , Eq. (10). The maximum broadening can be estimated as $\Omega_c^2/4\gamma_{31}$, see Eq. (11). The

values of γ_{broad} at zero detunings are given in Table 2. It is found that the broadening can be significant and exceed the natural line width by several orders of magnitude.

An aspect of interest in such investigations consists in determination of frequency shift and, therefore, refinement of the distances to the source of light and the sizes of cloud. The accuracy of the redshift determination is on the level of 10^{-10} [40], and reaches 10^{-11} in some cases [31]. The procedure of the redshift definition can be reduced to finding the maximum of the corresponding line contour. In the same way, the frequency shift was obtained, Eq. (15). The maximum frequency shift arises when $\delta_p + \delta_c = \gamma_{31}/2$. Numerical values are listed in Table 2 in the third column for the $\delta_{\text{shift}}^\beta$ and are γ_{broad} at maximums (see the second column of Table 2). So, the uncertainty of the redshift, δz_{shift} , can be estimated via frequency shift δ_{shift} :

$$\delta z_{\text{shift}} = \frac{\delta_{\text{shift}}(1 + z_{\text{abs}})}{\nu_0}, \quad (20)$$

where ν_0 is the transition frequency. The values given in Table 2 show that this effect is quite negligible and can be excluded from the corresponding analysis.

6. Conclusions

The paper studied the 21 cm line profile for the hydrogen atom within the framework of the density matrix formalism. Application of density matrix theory allows the detailed description of the emission/absorption processes when the atom is illuminated by the powerful source of light. The one-photon absorption line profile can be obtained in this case within the two-level approximation of atomic system, which represents the zeroth approximation. However, the additional emission/absorption processes should be taken into account. These processes can be evaluated within the three-level approximation. The additional interfering transitions were shown to lead to a substantial modification of the corresponding line profile.

Corrections to the frequency and level width were found. The frequency shift can be attributed to the redshift. Although the frequency shift is negligibly small, the width of line profile can be several orders larger than the natural one. The most significant effect arises for the optical depth. In particular, uncertainty of the optical depth determination is about 13% in case of J0414+0534 source, see Table 1, whereas correction Eq. (9) is on the order of 39%. The same result can be found for the 3C 49 light source: uncertainty and correction are about 8% and 20%, respectively. The magnitude of correction to the optical depth and, therefore, to the column density can be as high as 60%, see Table 2. In particular, when $z \approx z_{\text{abs}}$, fitting of the observed line profile with the one-photon isolated resonant contour can lead to the overestimation of the corresponding magnitudes.

Acknowledgments

This work was supported by Russian Science Foundation (grant 17-12-01035).

References

- [1] Kanekar N and Briggs F H 2004 *New Astron. Rev.* **48**, 1259
- [2] Laor A 1997 *Galactic Cluster Cooling Flows. ASP Conference Series* **115** 92 (arXiv: astro-ph/9609163)
- [3] Rauch M 1998 *Annu. Rev. Astron. Astrophys.* **36** 267
- [4] Rees M J 2000 *Phys. Rep.* **333-334** 203
- [5] Varshalovich D A 1967 *J. Exp. Theor. Phys. (USSR)* **52** 242 (Engl. Transl.: 1967 *Sov. Phys. JETP* **25** 157)
- [6] Boyd R W 2008 *Nonlinear Optics* (Orlando: Academic Press Third Edition)
- [7] Solov'yev D, Dubrovich V and Plunien G 2012 *J. Phys. B: At. Mol. Opt. Phys.* **45** 215001
- [8] Solov'yev D and Dubrovich V 2014 *Cent. Eur. J. Phys.* **12** 367
- [9] Whitley R M and Stroud R 1976 *Phys. Rev. A* **14** 1498
- [10] Gea-Banacloche J, Li Y-Q, Jin S-Z and Xiao M 1995 *Phys. Rev. A* **51**, 576
- [11] Wielandy S and Gaeta A L 1998 *Phys. Rev. A* **58** 2500
- [12] Sobolev V V 1957 *Soviet Astr.-AJ* **1** 678
- [13] Fox A J et al. 2009 *Astron. Astrophys.* **503** 731
- [14] Møller P, Fynbo J P U, Ledoux C and Nilsson K K 2013 *Mon. Not. R. Astron. Soc.* **430** 2680
- [15] Gupta N et al. 2006 *Mon. Not. R. Astron. Soc.* **373** 972
- [16] Curran S J et al. 2004 *Mon. Not. R. Astron. Soc.* **356** 1509
- [17] Abdo A A et al. 2010 *The Astrophys. J.* **716** 30
- [18] Kanekar N and Chengalur J N 2003 *Astron. Astrophys.* **399** 857
- [19] Curran S A *Catalogue of Damped Lyman Alpha Absorption Systems and Radio Flux Densities of the Background Quasars* (<http://www.phys.unsw.edu.au/~sjc/home/dla/>)
- [20] Curran S J et al. 2008 *Mon. Not. R. Astron. Soc.* **391** 765
- [21] Ishwara-Chandra C H et al. 2003 *J. Astrophys. Astr.* **24** 37
- [22] Vermeulen R C et al. 2003 *Astron. Astrophys.* **404** 861
- [23] Pihlstrom Y M et al. 2003 *Astron. Astrophys.* **404** 871
- [24] Tanna A et al. 2013 *ApJ* **772** L25
- [25] Curran S J et al. 2007 *Mon. Not. R. Astron. Soc.* **382** L11
- [26] Moore C B et al. 1999 *The Astrophys. J.* **510** L87
- [27] Cody A M and Braun R 2003 *Astron. Astrophys.* **400** 871
- [28] Chandra P et al. 2004 *J. Astrophys. Astr.* **25** 57
- [29] Labiano A et al. 2006 *Astron. Astrophys.* **447** 481
- [30] Andreani P et al. 2002 *Astron. Astrophys.* **381** 389
- [31] Wolfe A M et al. 2011 *The Astrophys. J.* **733** 24
- [32] Massardi M et al. 2008 *Mon. Not. Roy. Astron. Soc.* **384** 775
- [33] Michalitsianos G et al. 2009 *The Astrophys. J.* **474** 598
- [34] Turnshek D A and Bohlin R C 1993 *The Astrophys. J.* **407** 60
- [35] Rao S M and Turnshek D A 2000 *The Astrophys. J. Supp. S.* **130** 1
- [36] Taramopoulos A et al. 1995 *The Astronom. J.* **109** 480
- [37] Srianand r and Petitjean P 1998 *Astron. Astrophys.* **335** 33
- [38] Lu L et al. 1996 *The Astrophys. J. Supp. S.* **107** 475
- [39] Ledoux C, Bergeron J and Petitjean P 2002 *Astron. Astrophys.* **385** 802
- [40] Darling J 2012 *The Astrophys. J. Lett.* **761** L26
- [41] Curran S J et al. 2013 *Mon. Not. Roy. Astron. Soc.* **429** 3402